Direct Imaging of Stochastic Domain-Wall Motion Driven by Nanosecond Current Pulses

Guido Meier,* Markus Bolte, and René Eiselt
Institut für Angewandte Physik und Zentrum für Mikrostrukturforschung, Universität Hamburg, Jungiusstrasse 11, 20355 Hamburg, Germany

Benjamin Krüger
I. Institut für Theoretische Physik, Universität Hamburg, Jungiusstrasse 9, 20355 Hamburg, Germany

Dong-Hyun Kim
Department of Physics and Institute for Basic Research, Chungbuk National University, Cheongju 361-763, South Korea

Peter Fischer
Center for X-Ray Optics, Lawrence Berkeley National Lab, 1 Cyclotron Road, Mail Stop 2R0400, Berkeley, California 94720, USA
(Received 27 December 2006; published 2 May 2007)

Magnetic transmission x-ray microscopy is used to directly visualize the influence of a spin-polarized current on domain walls in curved permalloy wires. Pulses of nanosecond duration and of high current density up to 1.0×10^{12} A/m^2 are used to move and to deform the domain wall. The current pulse drives the wall either undisturbed, i.e., as composite particle through the wire, or causes structural changes of the magnetization. Repetitive pulse measurements reveal the stochastic nature of current-induced domain-wall motion.

DOI: 10.1103/PhysRevLett.98.187202 PACS numbers: 75.60.Ch, 68.37.Yz, 72.25.Ba, 75.60.Ej

Current-driven domain-wall (DW) dynamics paves the way to novel concepts for memory [1] and logic devices [2]. The underlying physics is still under debate [3–6]. Several models have been proposed to predict the effects of a spin-polarized electric current interacting with a locally inhomogeneous magnetization [3–5,7–11]. It was initially assumed that for DWs wider than the magnetic coherence length the spins of the conduction electrons adiabatically follow the local magnetic moments [4,12]. Later a nonadiabatic term was added [3,4,9] to account for the different DW velocities of theory and experiment [6,13]. It has be shown that the adiabatic term is largely responsible for the initial velocity of the DW while the nonadiabatic term controls its terminal velocity [3]. The velocity of magnetic DWs in thin nanowires has been stated to be between tenths of m/s [3,14,15] up to several 100 m/s [3,16,17]. The velocities reported by experiments tend to be less than those from theoretical predictions. Various suggestions have been proposed to account for this discrepancy, in particular, thermal activation [14,16,18,19] and surface roughness [16]. On the other hand, it has been found that the DW velocity depends on the DW type [14,20] and that a spin-polarized current can change the topology of a wall [14]. Moreover, it has been predicted that fast-changing currents should exert a force on a DW much stronger than the constant current alone [10] which implies that the time structure of the fast-changing current should be considered. Thus, to understand the underlying physics of current-driven DW motion it is required to determine the DW velocity and to simultaneously observe the DW type and topology as well as to accurately control the time structure of the current.

In this Letter we report spatially resolved experiments and micromagnetic simulations of the motion of vortex DWs in curved wires driven by current pulses. Nanosecond current pulses are used to determine the DW velocity. In case of microsecond pulses an average velocity including pinning and depinning of the wall might be measured. We show that DW velocities comparable to the field-driven case are obtained and that the current-driven motion follows a statistical distribution comparable to Barkhausen jumps in the field-driven case.

Curved wires with a radius of 25 μm were patterned by electron-beam lithography and lift-off processing from permalloy films deposited by electron-beam evaporation. Curved wires are most convenient for the field-controlled creation and destruction of a single DW. Four electrical contacts on each wire are patterned from a 60 nm thick Au layer for injection of current pulses and measurement of the dc impedance. Figure 1 shows an optical micrograph of a permalloy wire on a 100 nm thick Si_3N_4 membrane. The membrane is required for transmission soft x-ray microscopy. The distance between the two inner Au contacts is 4.2 μm.

Measurements of the anisotropic magnetoresistance (AMR) at low current densities of 1.0×10^9 A/m^2 prior to the pulse experiments provide full control over the field-induced generation of a single DW between the inner contacts. An example of an AMR measurement is depicted in Fig. 1(d). The resistance is lowest at saturation and highest at remanence, as expected [21]. For the pulse measurements we use the onion states with either a tail-to-tail or a head-to-head DW between the contacts depending on the magnetic history. From the absolute resist-

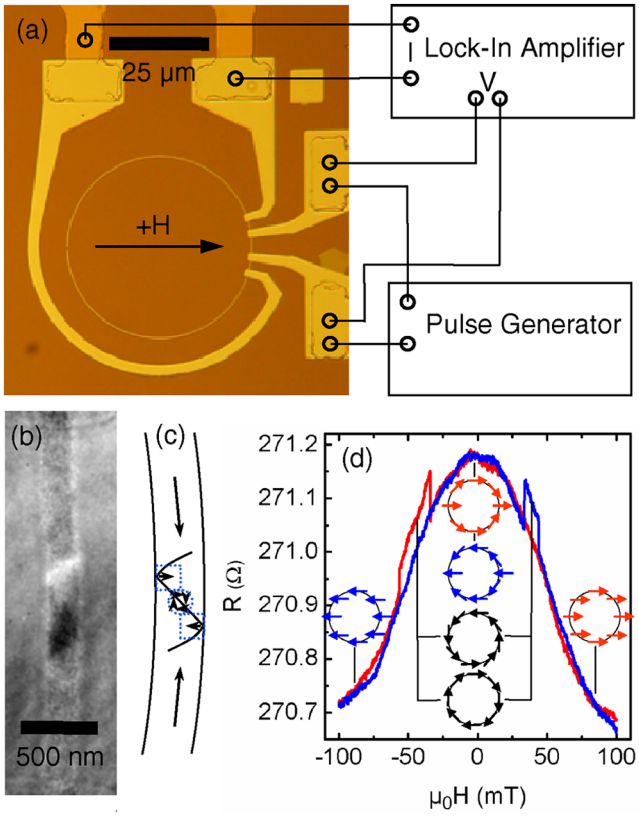

FIG. 1 (color online). (a) Optical micrograph of a curved permalloy wire on a Si_3N_4 membrane with four gold contacts. A slit on the left side avoids dc current flow through this part. (b) MTXM image and (c) scheme of a vortex wall in the section between the inner contacts. (d) Measured AMR. The up-sweep (down-sweep) is plotted in blue (red). The arrows indicate the magnetization states. Shown are schemes of the two saturated states, the two global-vortex states, and the two onion states. At remanence the onion states exhibit either a tail-to-tail (blue) or a head-to-head (red) DW in the region of interest for the pulse experiments.

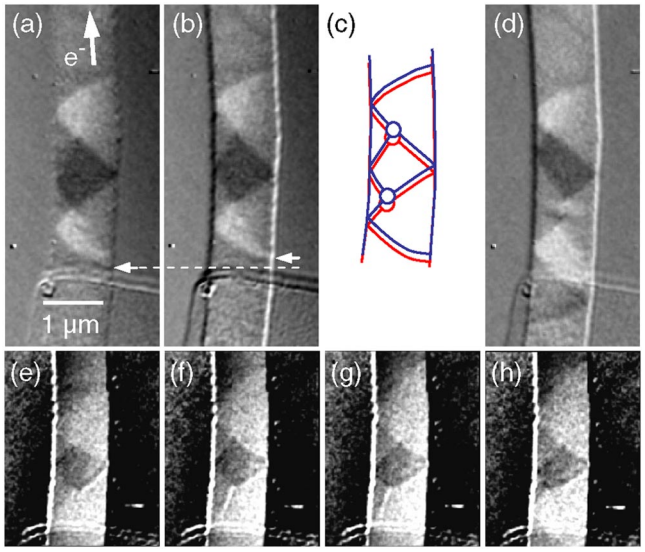

FIG. 2 (color online). (a) MTXM image of a double-vortex wall before and (b) after sending ten current pulses of 1.0 ns duration and 4.0 ns periodicity through the wire. (c) Sketch of the wall positions in (a) and (b) illustrating the motion of the double-vortex wall as composite particle. (d) Another pulse sequence generates a vortex-antivortex pair. (e)–(h) Sequence of MTXM images of a double-vortex wall taken after single 1.0 ns long current pulses with a current density of 1.0×10^{12} A/m^2. The lower vortex moves successively to the left edge of the wire.

ance at zero field, the geometry of the wire, and the distance between the voltage contacts we obtain a specific resistivity of 45 $\mu\Omega$ cm for the permalloy on the Si_3N_4 membrane. After the AMR characterization, magnetic transmission x-ray microscopy (MTXM) [22] with high lateral resolution down to 15 nm utilizing Fresnel zone optics [23] is used to image the magnetization of the wire. Figures 1(b) and 1(c) show an MTXM image and a scheme of a single-vortex wall, respectively.

Figure 2 shows MTXM images of double-vortex walls in the 960 nm wide wire. Prior to each image current pulses of 1.0 ns duration and a density of 1.0×10^{12} A/m^2 are sent through the wire in the direction indicated. In Fig. 2(a) and 2(b) the current-induced motion of a double-vortex wall in the direction of the conduction electrons is observed. Here, the wall moves with an undisturbed shape, i.e., as composite particle as predicted theoretically in Ref. [20]. A sketch of the motion is given in Fig. 2(c). However, in the repetitive pulse experiments also a current-induced distortion of the double-vortex wall is observed as vividly displayed in Fig. 2(d). Note that a vortex-antivortex pair has been created with the current pulse. Figures 2(e)–2(h) show MTXM images of a double-vortex wall which correspond to the results shown in Fig. 3. The current pulses successively move the lower vortex in a Barkhausen-like manner from pinning site to pinning site to the left, i.e., perpendicular to the direction of the conduction electrons.

It is well known that field-driven magnetization reversal is mediated via a sequence of Barkhausen jumps [24]. Disorder plays a significant role in the process of field-driven Barkhausen avalanches as there are pinning sites which cause a local distribution for the probability of DW depinning and motion [25]. We assume a similar mechanism in case of current-driven DW motion and expect a thermally activated process for the room temperature measurements with an energy barrier related to pinning by defects or to wall transformations at the wire borders as demonstrated in Ref. [16]. To analyze the stochastic nature of current-induced DW motion in more detail we have repeatedly imaged a double-vortex wall and sent current pulses of 1.0 ns duration, 100 ps rise time, and 7.5×10^{11} A/m^2 (1.0×10^{12} A/m^2) density through it. In the present experiment the DW width is much larger than the magnetic coherence length of the conduction electrons [11]. Thus the spins of the conduction electrons can follow the direction of the local magnetization [4,9] although the

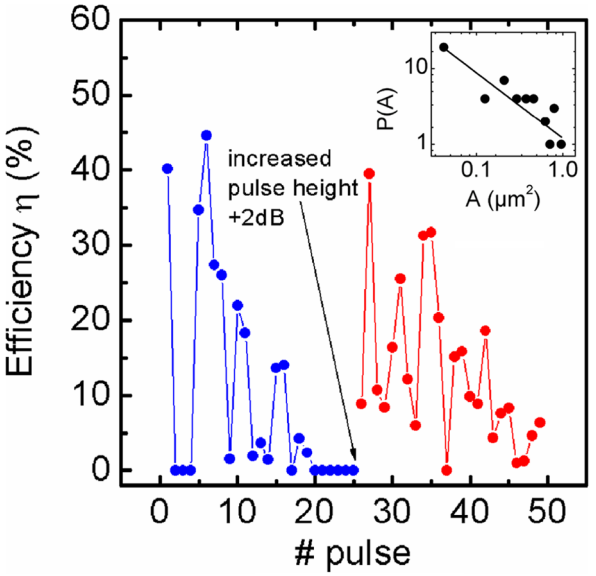

FIG. 3 (color online). Efficiency of DW displacement for 49 pulses of 1.0 ns duration. The current density of the pulses was increased from 7.5×10^{11} A/m^2 to 1.0×10^{12} A/m^2 after pulse No. 25.

nonadiabatic correction introduces an angle between the local magnetization and the magnetic moment of the conduction electrons. From the difference of two successive x-ray images the lateral area A in which the magnetization has been changed by one current pulse is determined. Following the approach of Ref. [6], the efficiency of DW displacement $\eta = \Delta m/m_{\text{current}}$, where $\Delta m = 2M_S Ad$ is the change of the magnetic moment in the wire and $m_{\text{current}} = 2P\mu_B wtj\Delta t/e$ is the magnetic moment carried by the current pulse, can be determined. The spin polarization of $P = 35\%$ is determined by point-contact Andreev spectroscopy [26]. With the thickness $d = 80$ nm and the width $w = 960$ nm of the wire, the saturation magnetization $M_S = 800$ kA/m^2, and the pulse duration $\Delta t = 1.0$ ns we calculate the efficiency plotted in Fig. 3 for 49 pulses and two different current densities. It clearly shows the stochastic nature of the process; e.g., for a number of pulses no motion of the DW is observed. We believe that the stochastic nature, i.e., a continuous pinning and depinning, is the reason for the extremely low DW velocities obtained from measurements with long current pulses [14]. It is interesting to compare the distribution $P(A)$ of the current-driven jump size A to the field-driven case of Barkhausen jumps. The inset of Fig. 3 shows a power-law behavior for $P(A)$ akin the field-driven case. The experimental data are fitted by $P(A) \propto A^{-\tau}$ with a critical exponent of $\tau = 0.9 \pm 0.2$. This exponent differs from the universality class for field-driven Barkhausen jumps in thin films of various thicknesses and materials [25]. However, for a final quantitative determination of the critical exponent the number of repetitions must be increased to improve the statistics.

To compare the experimental results with theory we implemented the spin-torque transfer model of Zhang and Li [3] in the micromagnetic framework OOMMF [27] and simulated the influence of current on a DW in curved wires [10]. Here, we apply this code to determine the current-induced DW velocity using the material parameters of permalloy, i.e., an anisotropy constant of $K = 100$ J/m^3, an exchange constant of $A = 1.3 \times 10^{-12}$ J/m, and a saturation magnetization of $M_S = 800$ kA/m, the Gilbert damping parameter $\alpha = 0.01$, the degree of nonadiabaticity $\xi = 0.01$, and the geometry of the approximately 1 μm wide wire of Fig. 2. Figure 4 shows the simulation of a double-vortex wall while a current of density 1.0×10^{12} A/m^2 is sent through the wire. The time difference between Figs. 4(a) and 4(b) is 1.0 ns. Taking the right end of the double-vortex wall as a measure for the motion one obtains a velocity of 110 m/s. A comparison with the experimental data in Fig. 2 reveals that the simulated and the measured static domain structure are consistent [28]. The current-induced DW velocities determined from simulation and experiment are also in good agreement. The simulated DW velocity is not homogeneous in time and space as DW motion occurs in jumps from pinning center to pinning center given by the edge roughness due to the discretization. A strong influence of the edge roughness of the wire on the DW velocity for the field-driven case is well known from the literature [16]. Furthermore, inner excitations of DWs are observed under the influence of the current, e.g., the generation of a vortex-antivortex pair, which is in turn annihilated under emission of spin waves (not shown). Thus micromagnetic simulations support the interpretation of the experimental results and underline the importance of the stochastic nature of current-driven DW motion [29].

In the following, we focus on the perpendicular motion of vortex cores observed repeatedly, e.g., in Fig. 2(e)–2(h).

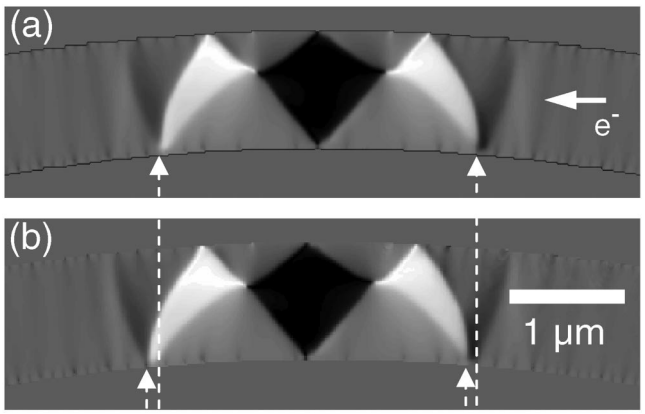

FIG. 4. Micromagnetic simulation of the influence of a spin-polarized current with a current density of 1.0×10^{12} A/m^2 on a double-vortex wall in a curved permalloy wire of 1 μm width and 80 nm thickness. The time difference between (a) and (b) is 1 ns. The right edge of the wall has moved 110 nm.

The perpendicular motion of a vortex core was calculated analytically and by micromagnetic simulation in Ref. [20]. There, the number of vortex cores was reduced by one from a vortex wall to a transverse wall. The description of the vortex motion by a restoring force, i.e., the coupling of vortices via a spring constant, can also be used to describe the more complex walls of the present experiments. The vortex polarity p determines to which edge of the wire the vortex moves. We deduce a perpendicular displacement y_0 of 83 ± 36 nm of the lower vortex core in Fig. 2 for a single 1.0 ns long current pulse of density 1.0×10^{12} A/m^2. If the deduced perpendicular displacement y_0 is applicable we can solve Eq. (21) of Ref. [20] and extract the ratio between the degree of nonadiabaticity ξ and the Gilbert damping parameter α

$$\frac{\xi}{\alpha} = 1 - \frac{\kappa y_0}{G_v b_j^c}, \tag{1}$$

where $\kappa = \frac{4K^{3/2}}{\pi\sqrt{A}}$ is the spring constant, $G_v = -\frac{2\pi M_S pt}{\gamma}$ the value of the gyrocoupling vector with the gyromagnetic ratio γ, the parameter of the current density $b_j^c = \frac{P j_c \mu_B}{e M_S (1+\xi^2)}$, and j_c the critical current density that moves the vortex to the next pinning site. In the present wire the anisotropy is comparable to the one of an extended film; i.e., the shape anisotropy is small, justifying the value of $K = 100$ J/m^3 in agreement with the phase diagram for DWs in nanowires [30]. Since $\xi^2 \ll 1$ we neglect this term in b_j^c and obtain $\xi = (0.96 \pm 0.02)\alpha$ in good agreement with the experiments of Ref. [17]. This evidences that the nonadiabatic spin-torque term is important for DW motion.

To exclude Joule heating [18] as a possible cause for DW motion we calculate the heat deposited by a single current pulse of 1.0 ns duration and 1.0×10^{12} A/m^2 current density from the sample geometry, the specific resistivity, and the heat capacity of permalloy. A temperature increase of 115 K is calculated which is considerably lower than the Curie temperature of permalloy (850 K) and room temperature where the experiments were performed. In the above estimate the heat flow through the wire is neglected; i.e., the calculated temperature increase is an upper limit that is in agreement with the detailed calculations of Ref. [31] that yield 68 K for our parameters. Thus we conclude that in the present experiments the motion of the DW is caused by the spin-transfer torque and is not much affected by Joule heating.

In conclusion, we have performed soft x-ray microscopy with high spatial resolution to image the current-induced motion of vortex-DWs in curved wires. Nanosecond current pulses were used to determine a DW velocity of 110 m/s which is in agreement with recent theories and is comparable to the case of field-driven motion. We found that the current-driven motion exhibits a statistical distribution like Barkhausen jumps for the field-driven case.

We thank Ulrich Merkt and Daniela Pfannkuche for fruitful discussions and the staff of CXRO and ALS, in particular, Ron Oort, Paul Denham, Bob Gunion, and Erik Anderson for their help with the experiments. Financial support of the Deutsche Forschungsgemeinschaft via the Sonderforschungsbereich 668 "Magnetismus vom Einzelatom zur Nanostruktur" and via the Graduiertenkolleg 1286 "Functional metal-semiconductor hybrid systems" is gratefully acknowledged. This work was supported by the U.S. Department of Energy under Contract No. DE-AC02-05-CH11231.

*Electronic address: meier@physnet.uni-hamburg.de

[1] S. S. P. Parkin, US Patent 309,6,834,005 (2004).
[2] D. A. Allwood *et al.*, Science **309**, 1688 (2005).
[3] S. Zhang and Z. Li, Phys. Rev. Lett. **93**, 127204 (2004).
[4] G. Tatara and H. Kohno, Phys. Rev. Lett. **92**, 086601 (2004).
[5] A. Thiaville *et al.*, Europhys. Lett. **69**, 990 (2005).
[6] A. Yamaguchi *et al.*, Phys. Rev. Lett. **92**, 077205 (2004).
[7] J. Slonczewski, J. Magn. Magn. Mater. **159**, L1 (1996).
[8] L. Berger, Phys. Rev. B **54**, 9353 (1996).
[9] X. Waintal and M. Viret, Europhys. Lett. **65**, 427 (2004).
[10] B. Krüger *et al.*, Phys. Rev. B **75**, 054421 (2007).
[11] Y. Tserkovnyak, H. J. Skadsem, A. Brataas, and G. E. W. Bauer, Phys. Rev. B **74**, 144405 (2006).
[12] Z. Li and S. Zhang, Phys. Rev. B **70**, 024417 (2004).
[13] D. Atkinson *et al.*, Nat. Mater. **2**, 85 (2003).
[14] M. Kläui *et al.*, Phys. Rev. Lett. **95**, 026601 (2005).
[15] T. Ono *et al.*, Science **284**, 468 (1999).
[16] Y. Nakatani *et al.*, Nat. Mater. **2**, 521 (2003).
[17] M. Hayashi *et al.*, Phys. Rev. Lett. **96**, 197207 (2006).
[18] A. Yamaguchi *et al.*, Appl. Phys. Lett. **86**, 012511 (2005).
[19] A. Yamaguchi *et al.*, Phys. Rev. Lett. **96**, 179904 (2006).
[20] J. He *et al.*, Phys. Rev. B **73**, 184408 (2006).
[21] M. Kläui *et al.*, Appl. Phys. Lett. **81**, 108 (2002).
[22] P. Fischer, Curr. Opin. Solid State Mater. Sci. **7**, 173 (2003).
[23] W. Chao *et al.*, Nature (London) **435**, 1210 (2005).
[24] H. Barkhausen, Z. Phys. **20**, 401 (1919).
[25] D.-H. Kim *et al.*, Phys. Rev. Lett. **90**, 087203 (2003).
[26] L. Bocklage *et al.*, J. Appl. Phys. (to be published).
[27] M. Donahue and D. Porter, National Institute of Standards and Technology Interagency Report No. NISTIR 6376, 1999.
[28] Note that the curvature of the wire with respect to the double-vortex wall is reversed between experiment and simulation. However, the curvature is small; i.e., the confining potential in the curved and in the straight wire are very similar.
[29] A simulated Oersted field of several mT perpendicular to the wire caused no DW motion.
[30] Y. Nakatani *et al.*, J. Magn. Magn. Mater. **290–291**, 750 (2005).
[31] C.-Y. You *et al.*, Appl. Phys. Lett. **89**, 222513 (2006).